

RSC Advances

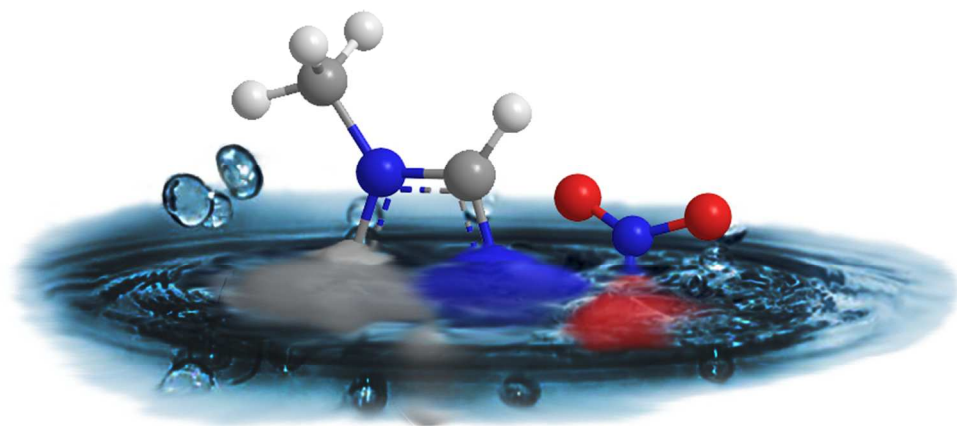


This is an *Accepted Manuscript*, which has been through the Royal Society of Chemistry peer review process and has been accepted for publication.

Accepted Manuscripts are published online shortly after acceptance, before technical editing, formatting and proof reading. Using this free service, authors can make their results available to the community, in citable form, before we publish the edited article. This *Accepted Manuscript* will be replaced by the edited, formatted and paginated article as soon as this is available.

You can find more information about *Accepted Manuscripts* in the [Information for Authors](#).

Please note that technical editing may introduce minor changes to the text and/or graphics, which may alter content. The journal's standard [Terms & Conditions](#) and the [Ethical guidelines](#) still apply. In no event shall the Royal Society of Chemistry be held responsible for any errors or omissions in this *Accepted Manuscript* or any consequences arising from the use of any information it contains.



80x39mm (300 x 300 DPI)

ARTICLE

Tuning of the freezing and melting points of [Hmim][NO₃] by the addition of water and nitrate salts

Cite this: DOI: 10.1039/x0xx00000x

Fabio Di Francesco,^{a,b,*} Carlo Ferrari,^c Letizia Moni,^a Bernardo Melai,^a Luca Bernazzani,^a Cinzia Chiappe^dReceived 16th June 2014,
Accepted 00th January 2014

DOI: 10.1039/x0xx00000x

www.rsc.org/

The fact that the physical and chemical properties of ionic liquids can be tailored is one of their key features. In most cases this is achieved by the appropriate selection of the cation and anion pair. In this paper we suggest that simple chemometric models can be used to describe various properties of these salts. We chose water and metal ions, generally considered as contaminants, to tune the melting and freezing points of a model ionic liquid, 1-methyl-imidazolium nitrate ([Hmim][NO₃]). Principal component analysis was used to select two representative metal ions (Li(I) and Cu(II)) on the basis of the charge and atomic radius of the cation, the crystallization water and the melting point of nitrate salt, which we believed would affect the behaviour of the [Hmim][NO₃]. A D-optimal design was used to plan the best experiments to obtain empirical models capable of predicting the melting and freezing points of this ionic liquid as a function of water and metal cation content.

Introduction

In the last twenty years ionic liquids (ILs) - low temperature molten salts exclusively composed of ions - have attracted the interest of a growing number of researchers in terms of their potential in both experimental and theoretical fields.¹ ILs have been proposed as solvents in several sectors, such as catalysis,² electrochemistry,³ lithium batteries,⁴ dye-sensitized solar cells,⁵ and lubricants⁶. Many ILs show interesting physical and chemical properties, such as a very low vapour pressure, a melting point below room temperature, wide liquid range, good conductivity, and good solvent power. The practically infinite combinations of cations and anions constituting ILs have led to high levels of tunability of their properties. The correlation between the systematic variations in the cation and/or anion structure of “pure” ILs and their physical and chemical properties has been systematically investigated, at least for the most commonly used ILs (mainly imidazolium salts), to accurately determine the relevant properties of these systems.⁷ There is considerable interest in the fluid properties of mixtures of ILs, ILs and molecular liquids or ILs and inorganic salts. Indeed, given that the desired properties can be obtained, the preparation of a mixture of ILs or the addition of a molecular liquid or salt to an IL is much easier and cheaper than the synthesis of a new functionalized pure IL.⁸ Often considered as an undesired contaminant, water can actually be used to modify

ILs' properties. Although classified as “hydrophobic”, many ILs absorb considerable amounts of water at room temperature.⁹ For example, N,N-octylmethylpyrrolidinium bis(trifluoromethanesulfonyl)imide ([ompyr][Tf₂N]) absorbed 0.7% moles of water when exposed for 5 min at 81% relative humidity.¹⁰

It is also well known that the addition of an inorganic salt can considerably change the physical and chemical properties of an IL.¹¹ For example, in one study the addition of LiBF₄ at concentrations above 0.5 M to 1-methyl-3-ethylimidazolium tetrafluoroborate ([emim][BF₄]) made the crystallization/melting peaks disappear, whereas the glass transition temperatures shifted to higher values with increasing LiBF₄ concentrations.¹² In addition, LiBF₄ decreased the ionic conductivity and the self-diffusion coefficients of the individual components of the IL, whereas the viscosity increased. A similar behavior of conductivity and viscosity as a function of lithium concentration has also been observed in the case of a lithium bis(trifluoromethanesulfonyl)imide/1,3-dimethyl-3-propylimidazolium bis(trifluoromethanesulfonyl)imide mixture¹³ and, more recently, of lithium bis(trifluoromethanesulfonyl)imide /N-alkyl-N-methylpyrrolidinium bis(trifluoromethanesulfonyl) imide.¹⁴

The ability to predict the effect of the addition of small amounts of inorganic salts on the properties of an IL or an IL mixture is very important for practical applications. Here, we report the

development of models describing the dependence of the melting and freezing points of a model ionic liquid, i.e. 1-methylimidazolium nitrate ([Hmim][NO₃]), on the concentration of additives such as inorganic nitrates, namely lithium nitrate and copper(II) nitrate, and water.

Melting and freezing points are important properties of ILs, which are strongly affected by the presence of dissolved molecular or ionic species. The relatively high melting point (about 60 °C) of pure [Hmim][NO₃] enabled us to investigate the effect of the additions without reaching particularly low temperatures. Principal component analysis was used to carefully choose the additives from commercially available inorganic nitrates. The use of salts with the same anion as the model IL limited any dissolution problems and enabled us to evaluate the effect of the addition of only the cation. A D-optimal design was used for the experiments, whose results were fitted to a simple quadratic model.

Experimental

Materials

1-Methylimidazolium nitrate was prepared by the dropwise addition of a 70% nitric acid aqueous solution (Sigma Aldrich) to equimolar methylimidazole (Sigma Aldrich, > 99%). The resulting solution was kept below 10 °C and stirred for 6 h. The excess water was removed under vacuum. The identity and purity of the product were then checked by NMR.

Lithium and copper nitrate were purchased from Sigma Aldrich.

Experimental Design

Experiments were designed according to a D-optimal design based on the D-criterion, i.e. maximization of the determinant of the information matrix ($X^T X$), where X is the model matrix.¹⁵ Fulfilling the D criterion leads to a maximum spread of the experiments in the experimental domain, so that a maximum volume is occupied and the experimental domain is explored to the maximum extent. This design is particularly helpful when the experimental region is not regular in shape or when the number of the experiments chosen by a classical symmetrical design is too large. The design of the experiments and calculations were carried out using dedicated software (Moddè, Umetrics).

The amount of water, expressed as mole/mole ratio of water to the IL, and the concentration of the metal cation, expressed as a mole/mole ratio of salt to the IL, were selected as model parameters. The effect of these additives was studied at three different levels, namely 0.0, 0.4 and 0.8 mol/mol of water and 0.0, 0.05 and 0.10 mol/mol of the metal cations respectively.

The following model was fitted to the data obtained from thermoanalytical measurements:

$$Y = \beta_0 + \beta_1 X_1 + \beta_2 X_2 + \beta_{11} (X_1)^2 + \beta_{22} (X_2)^2 + \beta_{12} X_1 X_2 \quad (1)$$

where X_1 is the concentration of the metal ion, X_2 is the concentration of water, and β_{nm} are the coefficients of the model. The model generated a surface of response describing the dependence of the melting and freezing points of the [Hmim][NO₃] on the concentration of the additives. More precisely, four experimental models were generated, two related to the copper salt (melting and freezing points) and two to the lithium salt. Each model was validated by verifying the accuracy of prediction at points far from those used to develop the model.

Sample Preparation

[Hmim][NO₃] and the inorganic salts were dried before use. The IL was heated to 60 °C in vacuum for 10 hours, and then kept under a nitrogen atmosphere. Lithium and copper nitrates were heated to 120 °C in vacuum for 24 h. A Karl-Fisher titration established that a 0.003 and 0.005 mol/mol of water remained after the drying procedures in [Hmim][NO₃] and in lithium nitrate respectively, whereas a 0.03 mol/mol of water was estimated in copper nitrate by thermogravimetric analysis (titration could not be used as copper reacts with the I₂/I₂ reagents). The maximum amount of “unwanted” water, i.e. water left in our mixtures after the drying procedures, was estimated at 0.006 mol/mol. The glassware used to prepare and contain the samples was heated for 4 hours at 120 °C to remove all traces of water, and then allowed to cool in a desiccator with silica gel. Each sample was prepared in a vial with a perforable septum by adding to about 1 g of [Hmim][NO₃] the appropriate amount of water and/or nitrate salt to the liquid. After each addition, the amount added was checked by weighing. The vials were then shaken and gently heated to favour the dissolution and homogenization of the sample. While still in the liquid state, the mixtures were quickly placed into an NMR tube whose open end was immediately welded by a blowtorch. Each sample was thus exposed to ambient air (relative humidity <50%) for just a few tens of seconds during the loading procedure and the welding of the tube.

Due to the small amounts of reagents used to prepare the samples, we were unable to perfectly follow the experimental plan (which resulted in a slight deformation of the experimental design). This shift from the ideal conditions was taken into account by modifying the design matrix from which the empirical model was then derived. The planned and actual compositions of the samples are reported in Table 1.

Table 1. Planned and actual compositions of samples

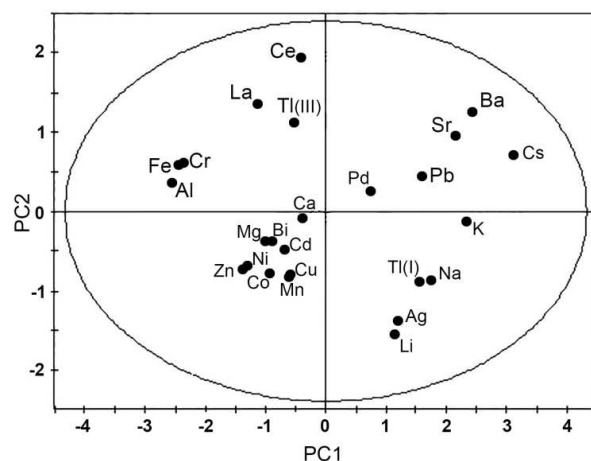
ID	Ion	Ion concentration (mol Me/ mol IL)		Water concentration (mol H ₂ O/ mol IL)	
		Planned	Actual	Planned	Actual
N1	Cu	0.00	0.00	0.00	0.00
N2	Li	0.00	0.00	0.00	0.00
N3	Cu	0.05	0.07	0.00	0.00
N4	Li	0.05	0.05	0.00	0.00
N5	Cu	0.10	0.14	0.00	0.00
N6	Li	0.10	0.11	0.00	0.00
N7	Cu	0.00	0.00	0.40	0.45
N8	Li	0.05	0.05	0.40	0.45
N9	Cu	0.10	0.14	0.40	0.41
N10	Cu	0.00	0.00	0.80	0.81
N11	Li	0.00	0.00	0.80	0.80
N12	Cu	0.05	0.07	0.80	0.79
N13	Li	0.05	0.08	0.80	1.02
N14	Cu	0.10	0.14	0.80	0.85
N15	Li	0.10	0.11	0.80	0.82
N16	Li	0.10	0.11	0.80	0.83
N17	Li	0.10	0.11	0.80	0.82
N18	Li	0.10	0.11	0.80	0.76

Thermal analysis

Thermal analysis was carried out by a home-made power compensation differential scanning calorimeter interfaced with a computer¹⁶. The calorimeter consisted of two twin (differential) calorimetric cells housing a reference NMR tube and an NMR tube containing about 350 mg of sample respectively. The power resolution was about 10 mW. The measurement procedure required a preliminary reference temperature scan with two empty NMR tubes, which was subtracted from the subsequent scans. Our calorimeter enabled temperature scans to be performed and the temperature¹⁷ to be modulated. In this study the modulation was not used and a calorimetric measurement only provided the value of the apparent specific heat, related to the heat flow generated or absorbed from the sample. The operating temperature range was -5 °C to 75 °C, with a scanning rate equal to 40 °C/h. The addition of copper nitrate gave rise to two melting points, and only the highest point corresponding to the complete melting of the sample was considered for the calculations. The relative standard deviation estimated from four replicate measurements was about 12% for the freezing point and 2% for the melting point. Since melting occurs at quasi-equilibrium conditions whereas crystallization takes place in a subcooled liquid (i.e. in a metastable state), such different dispersions of data are not surprising.

Results and Discussion

LiNO₃ and Cu(NO₃)₂ were chosen as representative additives on the basis of a principal component analysis (PCA). This technique, which does not require any a priori assumptions concerning the distribution of data, allows multidimensional data to be represented in a bidimensional plot (score plot). This result is achieved by a transition from an initial set of *m* generally correlated variables to another set of *n* (*n*<*m*) uncorrelated variables (principal components), which are obtained by linear combinations of the initial variables and are ordered according to the decreasing explained variance. The initial variables can be represented in terms of principal components on a second plot (loadings plot) which enables their mutual correlations to be studied (highly correlated variables are projected close to each another, anticorrelated variables are projected symmetrically with respect to the origin of axes). Parameters relevant to the nitrate salts, such as melting point and water crystallization molecules, and to their respective cations (charge, atomic radius) were included in the selection of additives. This is because they are considered to be significant in the IL-inorganic salt interaction and thus suspected to play a role in determining the shift of the melting and freezing points of [Hmim][NO₃]. In fact, the melting point of a salt depends on the compactness and stiffness of the crystal lattice, which are related to the sizes of the constituent atoms and their binding energy. The presence of water molecules or additional cations obviously affects the melting and freezing point of the [Hmim][NO₃]. If the unlikely formation of a system with complete miscibility within the solid is ruled out, a decrease in both points can be expected either from a thermodynamic point of view or by evaluating the stability of lattice and/or crystalline cells. The presence of water and/or inorganic salts should hinder the formation of a highly ordered lattice, resulting in a less compact and rigid structure. We hypothesized that the intensity of this perturbation was macroscopically related to the charge and size of the added cation, to its ability to form nitrate salts with a high melting point, and the presence of water crystallization molecules.



(a)

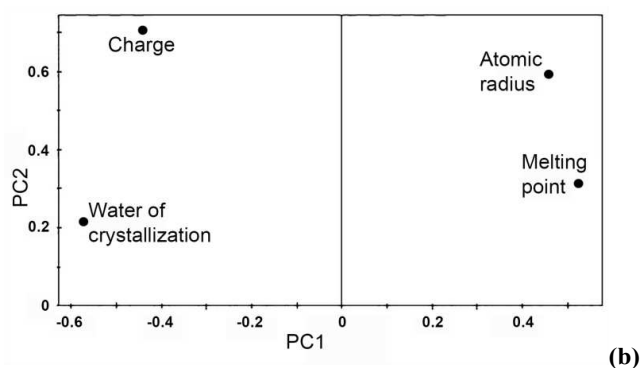


Figure 1. Principal component analysis of selected parameters related to commercial nitrate salts: **a)** score plot, **b)** loading plot.

The values of these parameters relevant to commercial nitrate salts that we used for PCA are reported in Table S.1.

The joint analysis of the score plot (Figure 1a) and the loading plot (Figure 1b) gives a more thorough interpretation of the PCA results. The first principal component appears to relate to the characteristics of nitrate salt (water crystallization molecules and melting point), and thus cations such as Al^{3+} , Cr^{3+} and Fe^{3+} on one side and Pd^{2+} , Pb^{2+} and K^{+} on the other side are plotted close to one another and in proximity of the x axis of the score plot. The second principal component seems to be more related to the characteristics of the cation, i.e. size and charge. This explains the position of cations such as Ce^{3+} , Tl^{3+} and La^{3+} on one side and Ag^{+} , Na^{+} and Li^{+} on the other. Ba^{2+} , Sr^{2+} and Cs^{+} are characterized by large atomic radii and a high melting point of the nitrate, whereas Mn^{2+} , Zn^{2+} and Co^{2+} show low levels of the same parameters. Salts with similar features lie close to each other on the score plot, and this information can thus be used to select representative salts with different features.

Based on this analysis, four representative nitrates (iron, barium, copper and lithium) located in different regions of the plots were selected. $\text{Cu}(\text{NO}_3)_2$ and LiNO_3 showed optimum solubility in $[\text{Hmim}][\text{NO}_3]$ during preliminary tests, and thus were chosen for subsequent experiments. Table 1 reports the experimental plan and the composition of the actual samples. The experiments were carried out in a random order.

Table 2. Experimental results: melting and freezing points determined by differential scanning calorimetry in the various experiments.

ID	Melting point (°C)	Freezing point (°C)
N1	64.5	52.3
N2	65.1	51.9
N3	56.2	39.6
N4	63.7	55.6
N5	40.6	9.0
N6	61.2	51.0
N7	48.8	31.4
N8	48.0	31.1
N9	30.1	-3.6
N10	37.0	15.3
N11	36.7	15.3
N12	32.5	7.1
N13	36.5	16.6
N14	17.1	-2.0
N15	35.7	16.2
N16	35.7	20.4
N17	36.5	21.0
N18	37.2	20.7

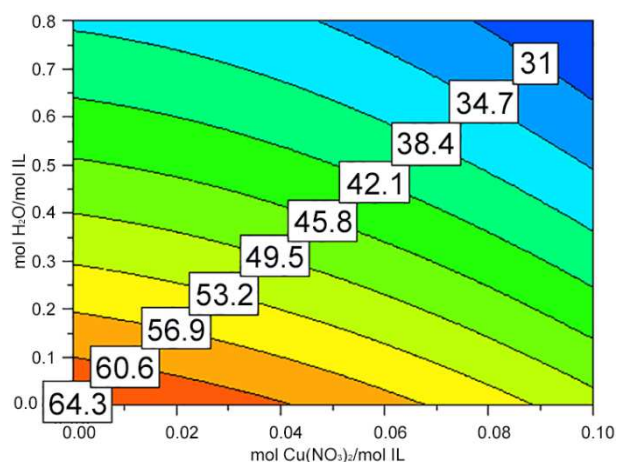
The melting and freezing points determined by differential scanning calorimetry are reported in Table 2. These data reveal that the addition of water (in our range of concentrations) has a more marked effect than the addition of salt, and that copper decreases the melting and freezing points more than lithium.

The melting points observed ranged from about 65 °C (pure ionic liquid) to 17 °C, when the highest amounts of water and copper were added. The corresponding freezing points were about 52 °C and -2 °C. Interestingly, a similarly low freezing point was obtained in experiment N9 (5.1 mol/mol of water and 0.13 mol/mol of copper) with a quite different melting point. The apparent increase in the freezing point in experiment N4 results from a combination of uncertainty in the measurement of this parameter and the negligible effect of the addition of a low amount of lithium. In all the “twin” experiments (copper vs lithium with the same concentrations), the shifts in both melting and freezing points obtained with lithium were lower than those obtained with copper.

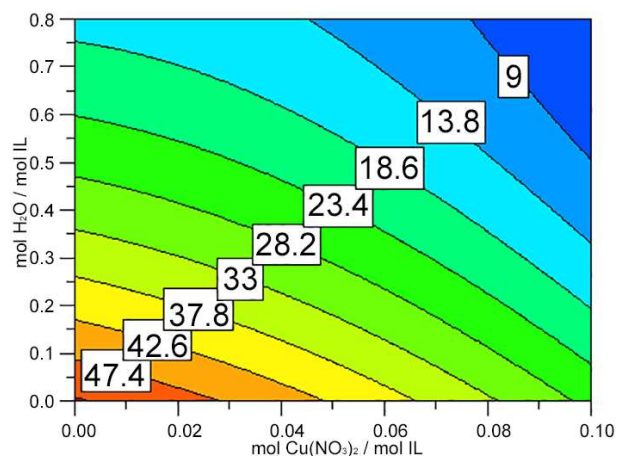
Figures 2 and 3 show the response surfaces related to the models describing the dependence of melting and freezing points on the composition of the mixture, whereas the coefficients of the models are reported in Table 3. As expected and previously seen from raw data, the presence of water or of an inorganic cation significantly decreases both the melting and freezing points.

Table 3. Coefficients to be inserted into Equation 1 to obtain the models that estimate the melting and freezing points of the mixtures.

Coefficient	Lithium		Copper	
	Melting point	Freezing point	Melting point	Freezing point
β_0	50.1	33.1	45.2	23.8
β_1	-0.6	0.8	-6.1	-9.7
β_2	-12.7	-18.0	-12.6	-14.5
β_{11}	-1.8	-2.4	-1.8	-2.4
β_{22}	1.8	3.9	1.8	3.9
β_{12}	0.8	3.2	0.8	3.2



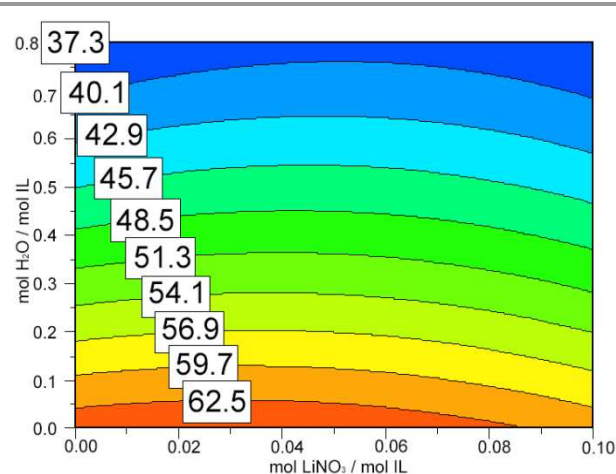
(a)



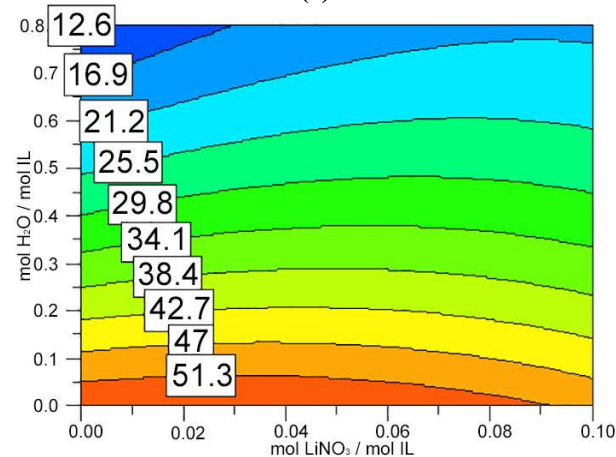
(b)

Figure 2. Contour plots representing the response surfaces describing the melting (a) and freezing point (b) of mixtures of [Hmim][NO₃], water and Copper(II) nitrate. Labels report temperature values for each isotherm.

In the investigated range, water has a more significant effect compared to the metallic cations.



(a)



(b)

Figure 3. Contour plots representing the response surfaces describing the melting (a) and freezing point (b) of mixtures of [Hmim][NO₃], water and lithium nitrate. Labels report temperature values for each isotherm.

This is evident from the absolute values of coefficients β_2 , which are larger than coefficients β_1 . In fact, this result is a consequence of investigating a much larger range of water concentrations than the range of cation concentrations. If the concentration of water is comparable to the concentration of metallic cation, copper has by far the largest effect, followed by water and then lithium. A synergic “water-metal cation” effect can be observed in the case of copper (II) which is not observed with lithium. Figure 4 shows DSC curves of pure [Hmim][NO₃] or [Hmim][NO₃] with added lithium or copper nitrate.

The samples containing lithium salt show a pattern of melting peaks compatible with a system with a partial miscibility within the solid phase and with the formation of a solid solution, whose maximum solid solubility at the eutectic temperature lies in the interval $0.05 < X_{Li} < 0.1$. This can be deduced from the presence of a small peak in the region around 25°C only in the samples with a high concentration of salt. This is likely due to the melting of an eutectic mixture.

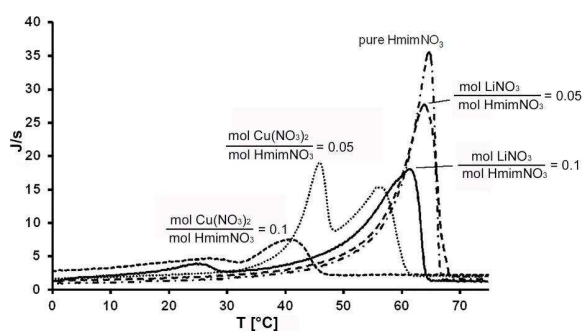


Figure 4. DSC curves of pure [Hmim][NO₃] and [Hmim][NO₃] added with different concentrations of lithium or copper nitrate.

When lithium nitrate was replaced with copper nitrate, there was a change in the shape of DSC curves with respect to both pure [Hmim][NO₃] and LiNO₃/[Hmim][NO₃] mixtures. Two distinct DSC peaks of a similar intensity appeared in the curve well below the melting temperature of pure IL. The position of these peaks shifted to lower temperatures and their intensity significantly decreased with a high copper salt concentration. In our experimental conditions this suggests the possible formation of a stable Cu(NO₃)₂/IL complex that gives rise to two eutectic mixtures. The reported ability of Cu(NO₃)₂ to form nitrocuprates ions in non-aqueous solvents supports this hypothesis¹⁸. However alternative hypotheses such as copper nitrate forming a 3D coordination polymer network or a metal-Hmim complex cannot be ruled out.^{19,20,21}

The prediction capability of the models was tested by performing two new experiments under significantly different conditions from those used for developing the model. A point in the center of the experimental domain was chosen for copper, whereas a point along one of the diagonals of the experimental domain was chosen for lithium, as the center of the domain had already been used to develop the model.

Table 4. Validation of the models: predicted and experimental values of melting and freezing points

Ion	Ion Concentration (mol Me/mol IL)	Water Concentration (mol H ₂ O/mol IL)	Melting Point (Pred.) (°C)	Melting point (Exp.) (°C)
Cu	0.07	0.4	42±3	40±1
Li	0.03	0.6	44±3	46±1

Ion	Ion Concentration (mol Me/mol IL)	Water Concentration (mol H ₂ O/mol IL)	Freezing Point (Pred.) (°C)	Freezing point (Exp.) (°C)
Cu	0.07	0.4	19±6	23±2
Li	0.03	0.6	24±6	27±2

The results of this validation are reported in Table 4, where confidence intervals of melting and freezing points were estimated from the replicate measurements included in the experimental plan in Table 1. The optimum agreement between predicted and experimental values demonstrated the validity of the models. A maximum unwanted amount of 0.006 mol/mol of water had been estimated by Karl-Fisher titration for our mixtures. The model allowed to assess that the maximum possible shifts of the melting and freezing points due to such water are 1 and 2 °C, which are within the uncertainty of the model.

Conclusions

We evaluated the effect of the addition of water and metal ions on the melting and freezing points of a model IL, [Hmim][NO₃]. The presence of water and nitrate salts led to a substantial decrease in the melting and freezing points of the IL. The use of an experimental plan based on a D-Optimal design enabled us to develop and validate four models for predicting the melting and freezing points as a function of water (up to 0.8 mol/mol) and lithium or copper (II) (up to 0.1 in mol/mol) content with a limited number of experiments.

The analysis of the response surfaces showed that in the investigated experimental range, the effect of water was greater than the metal cations. However, when concentrations were comparable, copper provided by far the largest effect, followed by water and then lithium.

A synergic effect between water and copper cation was observed, whereas this effect was negligible with lithium. A reasonable explanation for the different behaviour of copper may lie in the formation of a stable Cu(NO₃)₂/IL complex.

The development of models able to predict the melting point with an accuracy of about 5% and the freezing point with an accuracy of about 15% is the greatest strength of this study. This methodological approach was exceptionally successful, given the complexity of the observed phenomena, and could be extended in the future to other ILs and physical parameters. We believe that our results are also a further demonstration of the tunability of ionic liquids, one of the most successful features of these compounds in the field of Green Chemistry.

Notes and references

^a Dipartimento di Chimica e Chimica Industriale, via Risorgimento, Pisa, Italy. Fax: 39 050 2219660; Tel: 39 050 2219660; E-mail: jdifra@cci.unipi.it

^b Centro di ricerca "E. Piaggio", Largo Lucio Lazzarino 1, 56122 Pisa, Italy

^c Istituto Nazionale di Ottica - Consiglio Nazionale delle Ricerche UOS di Pisa "Adriano Gozzini" c/o Area della Ricerca CNR di Pisa

^d Dipartimento di Farmacia, Via Bonanno 33, 56126 Pisa, Italy

† **Electronic Supplementary Information (ESI)**

available: [Parameters relevant to commercial nitrate salts related to the Principal Component Analysis of Figure 1].

See DOI: 10.1039/b000000x/

- ¹ P. Wasserscheid and T. Welton, in *Ionic liquids in Synthesis*, Wiley–VCH, 2nd ed., Weinheim (Germany), 2008; N. V. Plechkova and K. R. Seddon, *Chem Soc. Rev.*, 2008, 37, 123; C. D. Hubbard, P. Illner and R. van Eldik, *Chem. Soc. Rev.*, 2011, 40, 272.
- ² J. P. Hallett and T. Welton, *Chem. Rev.*, 2011, 111, 3508.
- ³ H. Ohno, in *Electrochemical aspects of ionic liquid*, Wiley 6 Sons, Hoboken (New Jersey), 2nd ed., 2011.
- ⁴ G. T. Kim, S. S. Jeong, M. Z. Xue, A. Balducci, M. Winter, S. Passerini, F. Alessandrini and G. B. Appetecchi, *J. Power Source*, 2012, 199, 239.
- ⁵ Y. Zheng, Q. Huang, S. Fang, L. Yang and Y. Gan, *Int. J. Electroch. Sci.*, 2013, 8, 9558; L. J. Brennan, S. T. Barwich, A. Satti, A. Faure and Y. K. Gun'ko, *J. Mater. Chem. A*, 2013, 1, 8379.
- ⁶ A. E. Somers, P. C. Howlett, D. R. MacFarlane and M. Forsyth, *Lubricants*, 2013, 1, 3.
- ⁷ C. Chiappe and D. Pieraccini, *J. Phys. Org. Chem.*, 2005, 18, 275; M. Petkovic, K. R. Seddon, L. P. N. Rebelo and C. S. Pereira, *Chem. Soc. Rev.*, 2011, 40, 1383.
- ⁸ H. Niedermeyer, J. P. Hallett, I. J. Villar-Garcia, P. A. Hunt and T. Welton, *Chem. Soc. Rev.*, 2012, 41, 7780.
- ⁹ Y. Cao, X. Sun, Y. Chen, and T. Mu Sustainable; *Chem. Eng.*, DOI: 10.1021/sc4003246.
- ¹⁰ F. Di Francesco, N. Calisi, M. Creatini, B. Melai, P. Salvo and C. Chiappe, *Green Chem.*, 2011, 13, 1712.
- ¹¹ C. Chiappe, M. Malvaldi, *Phys. Chem. Chem. Phys.*, 2010, 12, 11191.
- ¹² K. Hayamizu, Y. Aihara, H. Nokagawa, T. Nukuda and W. S. Price, *J. Phys. Chem. B*, 2004, 108, 19527.
- ¹³ S. Seki, Y. Ohno, Y. Kobayashi, H. Miyashiro, A. Usami, Y. Mita, H. Tokuda, M. Watanabe, K. Hayamizu, S. Tsuzuki, M. Hattori and N. Terada, *J. Electrochem. Soc.*, 2007, 154, A173.
- ¹⁴ Q. Zhou, W. A. Henderson, G. B. Appetecchi, M. Montanino and S. Passerini, *J. Phys. Chem. B*, 2008, 112, 13577; O. Borodin, G. D. Smith and W. Henderson, *J. Phys. Chem. B*, 2006, 110, 16879.
- ¹⁵ deAguiar PF, Bourguignon B, Khots MS, Massart DL, PhanThanLuu R, *Chemometrics and Intelligent Laboratory Systems*, 1995, 30, 199; K. Smith, *Biometrika*, 1918, 1-2, 1.
- ¹⁶ G. Salvetti, C. Ferrari and E. Tombari, *Thermochim. Acta*, 1998, 316, 47.
- ¹⁷ E. Tombari, G. Salvetti, C. Ferrari, and G. P. Johari, *J. Phys. Chem. B*, 2007, 111, 496.
- ¹⁸ M. Rademeyer, *Acta Crystallographica*, 2006, E26, m259; G. Steinhausen, K. Karaghiosoff and T.M. Klapotke, *Z. Anorg. Allg. Chem.*, 2008, 634, 892.
- ¹⁹ V. I. Sokol, V. V. Davydov, N. Yu. Merkur'eva, V. S. Sergienko, O. A. Al-Saleh, Yu. V. Shklyae; *Russian Journal of Coordination Chemistry*, Vol. 31, No. 11, 2005, pp. 780–789. Translated from *Koordinatsionnaya Khimiya*, Vol. 31, No. 11, 2005, pp. 823–833.
- ²⁰ S. I. Troyanov, I. V. Morozov, K. O. Znamenkov, Yu. M. Korenev, "Synthesis and X-Ray Structure of New Copper(II) Nitrates: Cu(NO₃)₂•H₂O and β-modification of Cu(NO₃)₂" *Z. Anorg. Allg. Chem.* (1995) vol. 621, pp. 1261–1265.
- ²¹ R. E. LaVilla, S. H. Bauer; *J. Am. Chem. Soc.*, 1963, 85 (22), pp 3597–3600